# Laser-intensity requirements for generating enhanced kilovolt bremsstrahlung emission in intense laser-cluster interactions

K. G. Whitney, J. Davis, Tz. B. Petrova, and G. M. Petrov

Phys. Rev. A **85**, 063408 — Published 11 June 2012

DOI: 10.1103/PhysRevA.85.063408

# Laser Intensity Requirements for Generating Enhanced Kilovolt Bremsstrahlung Emission in Intense Laser-Cluster Interactions

K. G. Whitney*

*Berkeley Research Associates, 6551 Mid Cities Ave., Beltsville, MD, 20705, USA*

J. Davis, Tz. B. Petrova, and G. M. Petrov

*Naval Research Laboratory, Plasma Physics Division,*

*4555 Overlook Ave SW, Washington, DC 20375, USA*

## Abstract

The effects of ultra high intensity laser radiation on dynamical processes such as electron scattering, bremsstrahlung emission, pair production, etc. have recieved growing theoretical interest as laser intensities in the laboratory continue to increase. Recently, for example, a calculation was published that predicted more than four orders of magnitude resonant increases in bremsstrahlung emission in the presence of intense optical laser radiation [A. A. Lebed and S. P. Roshchupkin, Phys. Rev. A, 81, 033413 (2010)]. The analysis in this paper was limited to laser intensities $\leq 10^{17}$ W/cm$^2$, and it was applied only to bremsstrahlung emissions at the laser frequency. In the present paper, we extend this Lebed and Roshchupkin analysis in order to assess the possibility of achieving some enhancement to bremsstrahlung emissions at significantly higher harmonics of the optical laser photon energies ($\sim$ 6 keV) and thereby to appraise whether or not enhanced bremsstrahlung emissions may have played a hidden role in producing the population inversions and kilovolt x-ray amplifications that have been seen experimentally [A. B. Borisov, *et. al.*, J. Phys. B, 40, F307 (2007)]. In these experiments, light from a KrF laser was focused onto a gas of xenon clusters to intensities $\gtrsim 10^{19}$ W/cm$^2$. A model of the expansion and ionization dynamics of a xenon cluster when heated by such laser intensities has been constructed [Tz. B. Petrova, *et. al.*, High Energy Density Phys., 8, 209 (2012)]. It is capable of replicating the x-ray gains seen experimentally, but only under the assumption that sufficiently high inner-shell photoionization rates are generated in the experiments. We apply this model to show that such photoionization rates are achievable, but only if there are three to four orders of magnitude enhancements to the Bethe-Heitler bremsstrahlung emission rate. Our extended analysis of the Lebed and Roshchupkin work shows, for there to be emissions (enhanced by four orders of magnitude or not) at high order KrF-laser harmonic energies, that laser intensities $\gtrsim 10^{19}$ W/cm$^2$ must be reached. Thus, further extensions of these calculations (or experimental measusurements) are needed to detemine whether the enhancement factors that are predicted for small laser harmonics at laser intensities $\lesssim 10^{17}$ W/cm$^2$ can be extrapolated to large laser harmonics at laser intensities $\gtrsim 10^{19}$ , which are shown in our work to be needed in order to produce high laser harmonic kilovolt emissions.



* whitney@ppdmail.nrl.navy.mil

## I. INTRODUCTION

The relativistic calculation of the bremsstrahlung emission cross section in the absence of an external laser field has long been known and is well described in Ref. [1]. More recently, there has been a growing interest in the calculation of cross sections for bremsstrahlung emission and inverse bremsstrahlung absorption in the presence of intense laser fields[2–6]. In the presence of intense laser light ($I_{laser} \sim 10^{17}$ W/cm$^2$), for example, four or more orders of magnitude enhancements to the bremsstrahlung cross section have been predicted[2] for the special case of emission at the same frequency as the laser light. This result was derived under the restriction that the laser intensity was $\leq 10^{17}$ W/cm$^2$ so that, in particular, a lowest order Taylor series expansion of a Bessel function could be employed in the analysis and that alterations to the electron's 4-momenta could be ignored.

The development of ultra-high intensity KrF lasers, which have photon energies of 5 eV and intensities $\geq 10^{19}$ W/cm$^2$, has allowed experiments to be conducted in which x-ray amplification at 2.8 $\mathring{A}$ was observed[7] when a gas of xenon clusters was irradiated with intensities $\geq 10^{19}$ W/cm$^2$. Recently, in an attempt to determine whether the gain coefficient data that was inferred from these experiments could be modeled and thereby replicated theoretically, a time dependent molecular-plus-ionization dynamic xenon model was constructed[8, 10]. A key element in its development was the assumption that inner-shell photoionization processes dominate over inner-shell collisional processes in creating the hole states that produced the amplification. A second key element was the model's use of inner-shell photoionization rates shaped by Bethe-Heitler bremsstrahlung's density and temperature dependences and of magnitudes sufficient to produce the population inversions and gains that had been inferred from the experimental data. For these conditions on the size and shape of the photoionization rates to be satisfied, photon fluxes at and above 5.6 keV have to be of sufficient magnitude, in turn, to produce these large and needed photoionization rates. A promising source for such fluxes was thought to be enhanced bremsstrahlung emission in the presence of intense laser light, which is the photon source investigated in this paper. For such enhanced emissions to be theoretically feasible, two extensions of the calculations described in Ref. [2] are needed, one of which is described in this paper: namely, the extension of the theory to much higher harmonics of the fundamental laser frequency.

The bremsstrahlung cross-section calculations of Ref. [2] must also be extended to higher laser intensity levels at which the size of a dimensionless parameter, $\eta_0$, approaches and begins to exceed one. An exact semi-classical calculation of the bremsstrahlung cross section in the presence of an intense light field is difficult to carry out for a variety of reasons that are described in the formulation of the problem given in Refs.[2–4]. In this paper, therefore, we will calculate an enhancement factor for values of $\eta_0$ less than, but approaching, one, leaving open the question as to whether such enhancements remain intact as $\eta_0 \to 1$. The main focus of this paper is on the more limited problem of extending the analysis of Ref.[2] to determine the laser intensity requirements that would be needed to produce enhanced bremsstrahlung emissions at high KrF-laser frequency harmonics above 5.6 keV. As noted in Ref. [2], the amount of enhanced kilovolt emission is a quantity ultimately to be determined by experiment. Bessel function theory suggests that enhancements out to kilovolt energies are possible. Finally, therefore, a power output versus input argument is used to show that three to four orders of magnitude enhancements of the bremsstrahlung emissions at $I_{laser} \geq 10^{19}$ W/cm$^2$ would be sufficient to produce the required inner-shell photoionization rates needed to produce the observed x-ray amplification. The combined molecular and ionization dynamics model described in Refs. [9, 10] is employed to make this demonstration.

This paper is structured, therefore, as follows. In Section II, the preliminaries to a semi-classical bremsstrahlung calculation are taken intact from Ref. [2]. In this formulation of the bremsstrahlung problem, $\eta_0$-modifications to the electron's initial and final 4-momentum, which are described in Ref. [3], are ignored and the limitation that $\eta_0 \lesssim 0.3$ is implicitly assumed. In Section III, the formula for the bremsstrahlung emission cross section in the absence of an intense laser field is then extracted from this formalism as prelude to a repeat of this calculation in the presence of an intense laser field. In each of these cross-section calculations, four terms are to be evaluated, arising from the two lowest-order bremsstrahlung S-matrix elements. As was done in Ref.[2], however, we focus on the calculation of just one of these terms, and, as in Ref.[2], we average the cross-sections over electron spin and photon polarization. In the absence of laser light, this averaging leads to the evaluation of a trace over the product of four Dirac gamma matrices. In the presence of laser light, on the other hand, this same calculation also involves traces over the product of six and eight gamma matrices in addition to the trace over the product of four gamma matrices. The evaluations of these traces contain 15, 105, and 3 terms respectively. For simplicity, therefore, only terms

involving four gamma matices are computed. These calculations allow a formula for the chosen cross-section term to be derived in Section IV for kilovolt bremsstrahlung emissions that reduces, as it should, to the cross section term that is calculated in the absence of a laser field. The cross section in the presence of laser light contains Bessel functions whose arguments are functions of unrestricted laser field strengths. A comparison of these two cross-section terms then allows an estimate of the enhancement factor for bremsstrahlung emission in the presence of an intense laser field to be computed for values of $\eta_0 \lesssim 0.5$. Theoretically, it is an open question as to how this enhancement holds up as $\eta_0 \to 1$ and corrections to the initial and final 4-momenta of the electron enter the calculation in addition to the above mentioned neglected terms.

We address this question in Section V in a different set of calculations, which give indirect supporting theoretical evidence for the existence of enhanced bremsstrahlung emission in an intense laser field. The combined molecular/ionization dynamic model of Refs. [9, 10] is used in this section to compute the dynamical response of a xenon cluster of 200 atoms to an intense pulse of KrF laser radiation that is taken to peak at an intensity of $2 \times 10^{19}$ W/cm$^2$, which is comparable to the intensities achieved in the experiments of Ref.[7]. In a molecular dynamics calculation, average electron and ion densities and effective electron and ion temperatures are first calculated in response to this KrF pulse. These quantities are then used as input to an ionization dynamics calculation in which photoionization rates were chosen to correlate with the field-free bremsstrahlung emission rate and that were taken to have a peak value that produces the population inversions and the x-ray amplifications at $2.8\ \mathring{A}$ that were measured in the experiments[7]. Using these rates, one computes a photoionization power input to the cluster. It is found to compare favorably to the enhanced (by a factor of $4.5 \times 10^3$) field-free bremsstrahlung power output that is calculated using the averaged temperatures and densities derived from the molecular dynamics calculation. Finally, this work is summarized in Section VI.

## II. BREMSSTRAHLUNG EMISSION IN THE PRESENCE OF AN INTENSE LASER FIELD

### A. Preliminaries

In this section, a brief summary is given of a slightly revised version of the semi-classical theory of bremsstrahlung emission in the presence of an intense laser field that is given in Ref. [2]. As was noted in Ref. [2], two dimensionless parameters, $\eta_0$ and $\gamma_0$, play important roles in the bremsstrahlung analysis that follows:

$$\eta_0 \equiv \frac{eF_0}{m_0c^2}\frac{1}{k}, \qquad \gamma_0 \equiv \eta_0\frac{m_0c^2\beta_i}{\hbar\omega} = \frac{eF_0\beta_i}{\hbar\omega}\frac{1}{k}. \tag{1}$$

Here, $k = \omega/c$ is the laser wave number, $F_0$ is the electric field strength at the peak of the laser pulse, $m_0$ and $e$ are respectively the electron mass and charge, and $\beta_i = v_i/c$ is the electron velocity relative to the speed of light. $F_0$ and $\eta_0$ are given in terms of the peak laser intensity, $I^{max}_{\ell aser}$, by

$$F_0\left[\frac{statvolt}{cm}\right] = \sqrt{\frac{8\pi}{c}I^{max}_{\ell aser}} = 9.156\times10^{-2}\sqrt{I^{max}_{\ell aser}\,[W/cm^2]},$$
$$\eta_0 = 2.12\times10^{-10}\sqrt{I^{max}_{\ell aser}\,[W/cm^2]}. \tag{2}$$

Thus, for example, when $I^{max}_{\ell aser} = 10^{19}$ W/cm$^2$, $\eta_0 = 0.67$ and $F_0 = 8.69\times10^{10}$ V/cm.

As in Refs. [1] and [2], relativistic units in which $\hbar = c = 1$ are used in this paper and 4-vector scalar products are taken to be given by $(ab) \equiv a_0b_0 - \mathbf{a}\cdot\mathbf{b}$. Also, as in Ref. [2], the classical laser field is represented by the vector potential (describing circularly polarized light for its simplicity in this analysis),

$$A(\varphi) = \frac{F_0}{\omega}g\Big(\frac{\varphi}{\omega\tau}\Big)\big(e_x\cos\varphi + e_y\sin\varphi\big), \tag{3}$$

where

$$\varphi \equiv (kx) = \omega(t-z), \qquad k \equiv (\omega,\vec{k}) = \omega(1,0,0,1) \equiv \omega n \tag{4}$$

and

$$e_x \equiv (0,\mathbf{e}_x), \equiv (0,1,0,0), \qquad e_y \equiv (0,\mathbf{e}_y), \equiv (0,0,1,0),$$
$$e_x^2 \equiv (e_xe_x) = e_y^2 = -1, \qquad (e_xk) = (e_yk) = 0. \tag{5}$$

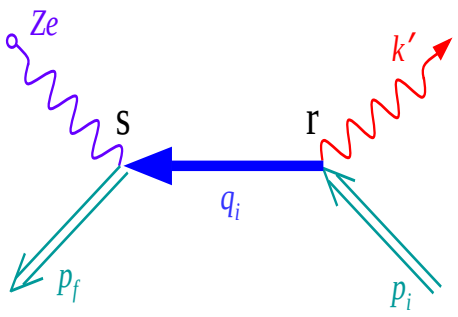


FIG. 1. The Feynman diagram depicting the electron bremsstrahlung emission assisted by an r laser photon absorption that is followed by the scattering of the electron from an ion of charge, Ze, and the absoption or emission of s laser photons.

Similar to the definition of the four vector $n = (1, 0, 0, 1) \equiv (1, \hat{n})$, where $\hat{n} = (0, 0, 1) = e_z$, we will also use the notation, $k' \equiv \omega' n' \equiv \omega'(1, \hat{n}')$.

In Ref. [1], the envelope function of the laser pulse, $g$, was taken to have an exponential fall-off: $g_{LR}(\phi) \equiv \exp(-4\phi^2)$, where $\phi \equiv \varphi/(\omega\tau) = (t - z)/\tau$ and $\tau$ is the laser pulsewidth.

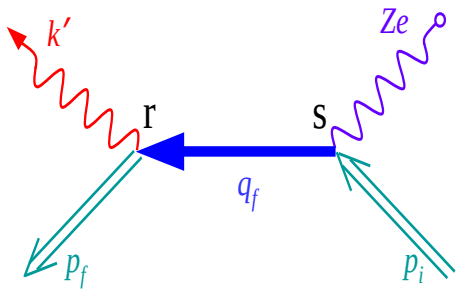


FIG. 2. The Feynman diagram depicting the electron bremsstrahlung emission assisted by an r laser photon absorption that follows the scattering of the electron from an ion of charge, Ze, with the absoption or emission of s laser photons.

However, for mathematical expediency, in this paper, $g$ is taken to be a square-wave pulse:

$$g(\phi) = g_0\eta_+(\phi + 1/2)\Big(1 - \eta_+(\phi - 1/2)\Big), \tag{6}$$

where $\eta_+(\phi) = 1$ when $\phi > 0$; $\eta_+(\phi) = 1/2$ when $\phi = 0$; and $\eta_+(\phi) = 0$ when $\phi < 0$. Note that by taking $g_0 = \sqrt{\pi}/2 = 0.886$, the areas under both envelope curves, $g_{LR}$ and $g$, are the same: $\int_{-\infty}^{\infty} d\phi g_{LR} = \int_{-\infty}^{\infty} d\phi g = \sqrt{\pi}/2$. With this choice of envelope function, Bessel

functions, $J_n$, of argument $g\gamma$ also become square wave functions and can be written as

$$J_n(g\gamma) = J_n(g_0\gamma)\eta_+(\phi+1/2)\Big(1-\eta_+(\phi-1/2)\Big) + \delta_{n0}\Big(1+\eta_+(\phi-1/2)-\eta_+(\phi+1/2)\Big). \quad (7)$$

This latter term is present because $J_n(0) = \delta_{n0}$. However, its presence in the following analysis can be ignored, so that

$$J_n(g\gamma) = J_n(g_0\gamma)\eta_+(\phi+1/2)\Big(1-\eta_+(\phi-1/2)\Big). \quad (8)$$

is employed in each of the following calculations.

In the semi-classical QED theory described in Ref. [2], the momentum transfer, $q_i$, at each of the two vertices in Fig. 1 includes contributions from $r$ and $s$ laser photons, respectively:

$$q_i = p_i - k' + rk, \quad (9)$$

$$q_i = p_f - q + sk, \quad (10)$$

The 4-vectors, $p_i$ and $p_f$ are the initial and final 4-momentum vectors of the scattered electron respectively, $k'$ and $k$ are the 4-momentum of the bremsstahlung and laser photons, respectively, and $q = (q_0, \vec{q})$ is the 4-momentum transfered to the ion off of which the electron is scattered. Note that

$$p_i = (E_i, \vec{p}_i), \qquad p_f = (E_f, \vec{p}_f), \qquad k' = \omega'(1, \hat{n}'), \qquad k = \omega(1, \hat{n}), \quad (11)$$

where

$$p_i^2 = E_i^2 - \vec{p}_i \cdot \vec{p}_i = m_0^2, \qquad k'^2 = \omega'^2(1 - \hat{n}' \cdot \hat{n}') = 0 = k^2. \quad (12)$$

Taken together the $q_i$ energy-momentum relations imply

$$q = p_f - p_i + k' + (s-r)k. \quad (13)$$

But because the ion is taken to be infinitely heavy in bremsstrahlung calculations, it absorbs effectively no energy from the scattering and therefore,

$$q_0 = E_f - E_i + \omega' + (s-r)\omega = 0, \quad (14)$$

from which equation, one derives the bremsstrahlung energy conservation relation,

$$\omega' = E_i - E_f + (r-s)\omega. \quad (15)$$

Thus, in the presence of an intense laser field, a bremsstrahlung photon can acquire its energy either entirely from the electron, entirely from the laser field in the form of a laser harmonic, or from a combination of the two. Likewise, in the exchange reaction depicted in Fig. 2, we have that

$$q_f = p_f + k' - rk, \tag{16}$$

$$q_f = p_i + q - sk, \tag{17}$$

which again implies that

$$q = p_f - p_i + k' + (s - r)k. \tag{18}$$

and that

$$\omega' = E_i - E_f + (r - s)\omega. \tag{19}$$

### B. Semi-classical S-matrix theory

We begin our analysis with the formula given in Ref. [2] for the S-matrix element for the scattering of an electron in the field of a heavy, stationary ion that results in the absorption or emission of $r-s$ photons from the laser field and the emission of a bremsstrahlung photon. Semi-classically,

$$S_{fi} \to S_{rs}^{fi}, \quad \text{where } -\infty < r < \infty, \quad -\infty < s < \infty, \tag{20}$$

and

$$S_{rs}^{fi} = -\imath \frac{Ze^3\sqrt{\pi}}{\sqrt{2\omega' E_f E_i}} \overline{u}_f (B_{rsi} + B_{rsf}) u_i, \tag{21}$$

where $u_f$ and $u_i$ are Dirac spinors for the final and initial states of the scattered electron and, from Ref. [2],

$$B_{rsi} = \frac{2\omega}{\mid \vec{q} \mid^2 + q_0(q_0 - 2q_z)} \int_{-\infty}^{\infty} d\xi \frac{\Lambda_s^{(1)}(\xi)(\hat{q}_i + m_0 + \hat{k}\xi)\Lambda_{-r}^{(2)}(\ xi)}{q_i^2 - m_0^2 + 2(kq_i)\xi}, \tag{22}$$

$$B_{rsf} = \frac{2\omega}{\mid \vec{q} \mid^2 + q_0(q_0 - 2q_z)} \int_{-\infty}^{\infty} d\xi \frac{\Lambda_{-r}^{(3)}(\xi)(\hat{q}_f + m_0 + \hat{k}\xi)\Lambda_s^{(4)}(\ xi)}{q_f^2 - m_0^2 + 2(kq_f)\xi}. \tag{23}$$

The matrix functions, $\Lambda_s^{(1)}(\xi), \cdots, \Lambda_s^{(4)}(\xi)$, are defined by

$$\Lambda_s^{(1)}(\xi) = \tau \int_{-\infty}^{\infty} d\phi \widetilde{\gamma}_0 \mathfrak{L}_s(\phi \mid \chi_{p_f q_i}, \gamma_{p_f q_i}) \exp\Big[\imath\Big(q_0 - \xi\omega\Big)\tau\phi\Big], \tag{24}$$

$$\Lambda^{(2)}_{-r}(\xi) = \tau \int_{-\infty}^{\infty} d\phi' \mathfrak{F}_{-r}(\phi' \mid \chi_{q_i p_i}, \gamma_{q_i p_i}) \exp\Big[\imath\Big(\xi\omega\tau\Big)\phi'\Big], \tag{25}$$

$$\Lambda^{(3)}_{-r}(\xi) = \tau \int_{-\infty}^{\infty} d\phi' \mathfrak{F}_{-r}(\phi' \mid \chi_{p_f q_f}, \gamma_{p_f q_f}) \exp\Big[\imath\Big(\xi\omega\tau\Big)\phi'\Big], \tag{26}$$

$$\Lambda^{(4)}_{s}(\xi) = \tau \int_{-\infty}^{\infty} d\phi \widetilde{\gamma}_0 \mathfrak{L}_{s}(\phi \mid \chi_{q_f p_i}, \gamma_{q_f p_i}) \exp\Big[\imath\Big(q_0 - \xi\omega\Big)\tau\phi\Big] \tag{27}$$

and the functions, $\mathfrak{L}_s(\phi \mid \chi_{p_f q_i}, \gamma_{p_f q_i}), \cdots, \mathfrak{L}_s(\phi' \mid \chi_{q_f p_i}, \gamma_{q_f, p_i})$, by

$$\mathfrak{L}_s(\phi \mid \chi_{p_f q_i}, \gamma_{p_f q_i}) \equiv \exp\Big(-\imath s \chi_{p_f q_i}\Big) J_s(\gamma_{p_f q_i}), \tag{28}$$

$$\mathfrak{F}_{-r}(\phi' \mid \chi_{q_i p_i}, \gamma_{q_i p_i}) \equiv \Big[\hat{\epsilon}^* J_{-r}(\gamma_{q_i p_i}) + (e_+ b) \exp\Big(-\imath \chi_{q_i p_i}\Big) J_{1-r}(\gamma_{q_i p_i})\Big] \exp\Big[\imath r \chi_{q_i p_i}\Big], \tag{29}$$

$$\mathfrak{F}_{-r}(\phi' \mid \chi_{p_f q_f}, \gamma_{p_f q_f}) \equiv \Big[\hat{\epsilon}^* J_{-r}(\gamma_{p_f q_f}) + (e_+ b') \exp\Big(-\imath \chi_{p_f q_f}\Big) J_{1-r}(\gamma_{p_f q_f})\Big] \exp\Big[\imath r \chi_{p_f, q_f}\Big], \tag{30}$$

$$\mathfrak{L}_s(\phi \mid \chi_{q_f p_i}, \gamma_{q_f p_i}) \equiv \exp\Big(-\imath s \chi_{q_f p_i}\Big) J_s(\gamma_{q_f p_i}) \tag{31}$$

where

$$e_+ \equiv e_x + \imath e_y, \qquad \hat{\epsilon}^* \equiv (\epsilon^* \widetilde{\gamma}), \tag{32}$$

$$b \equiv \frac{1}{4} \eta_0 g(\phi') m_0 \left( \frac{\hat{\epsilon}^* \hat{k} \widetilde{\gamma}}{(k p_i)} + \frac{\widetilde{\gamma} \hat{k} \hat{\epsilon}^*}{(k q_i)} \right), \qquad b' \equiv \frac{1}{4} \eta_0 g(\phi') m_0 \left( \frac{\hat{\epsilon}^* \hat{k} \widetilde{\gamma}}{(k p_f)} + \frac{\widetilde{\gamma} \hat{k} \hat{\epsilon}^*}{(k q_f)} \right), \tag{33}$$

$$\chi_{p_f, q_i} \equiv \arctan\left( \frac{(e_y Q_{p_f q_i})}{(e_x Q_{p_f q_i})} \right), \qquad \chi_{q_i p_i} \equiv \arctan\left( \frac{(e_y Q_{q_i p_i})}{(e_x Q_{q_i p_i})} \right). \tag{34}$$

$$\gamma_{p_f q_i} \equiv \eta_0 g(\phi') m_0 \sqrt{(e_x Q_{p_f q_i})^2 + (e_y Q_{p_f q_i})^2} \equiv g(\phi') \gamma'_{p_f q_i}, \tag{35}$$

$$\gamma_{q_i p_i} \equiv \eta_0 g(\phi') m_0 \sqrt{(e_x Q_{q_i, p_i})^2 + (e_y Q_{q_i, p_i})^2} \equiv g(\phi') \gamma'_{q_i p_i} \tag{36}$$

and

$$Q_{p_f q_i} \equiv \frac{p_f}{(k p_f)} - \frac{q_i}{(k q_i)}, \qquad Q_{q_i p_i} \equiv \frac{q_i}{(k q_i)} - \frac{p_i}{(k p_i)}. \tag{37}$$

Four-vector quantities with hats over them represent 4-vector dot products with the Dirac gamma matrices, e.g.,

$$\hat{q}_i \equiv q_i^\mu \widetilde{\gamma}_\mu = q_0 \widetilde{\gamma}_0 - \vec{q} \cdot \vec{\widetilde{\gamma}} \equiv \Big(q_i \widetilde{\gamma}\Big), \qquad \widetilde{\gamma}_\mu \equiv \Big(\widetilde{\gamma}_0, \widetilde{\gamma}_1, \widetilde{\gamma}_2, \widetilde{\gamma}_3\Big). \tag{38}$$

As can be seen from Eqs. (22)-(37), the analyses of $B_{rsi}$ and $B_{rsf}$ proceed along similar lines, and thus, as in Ref. [2], we focus principally on the analysis of $B_{rsi}$. Using Eq. (8), one can rewrite Eq. (28), for example, as

$$\mathfrak{L}_s(\phi \mid \chi_{p_f q_i}, \gamma_{p_f q_i}) = \exp\Big(-\imath s \chi_{p_f q_i}\Big) J_s(g_0 \gamma'_{p_f q_i}) \eta_+(\phi + 1/2) \Big(1 - \eta_+(\phi - 1/2)\Big) \tag{39}$$

and thus evaluate Eq. (24) as

$$\Lambda_s^{(1)}(\xi) = \tau\widetilde{\gamma}_0 \exp\Big(-\imath s\chi_{p_f q_i}\Big) J_s\Big(g_0\gamma'_{p_f q_i}\Big) \int_{-1/2}^{1/2} d\phi \exp\Big[\imath\Big(q_0 - \xi\omega\Big)\tau\phi\Big]$$
$$= \widetilde{\gamma}_0 \exp\Big(-\imath s\chi_{p_f q_i}\Big) J_s\Big(g_0\gamma'_{p_f q_i}\Big) \frac{2}{\Big(q_0 - \xi\omega\Big)} \sin\left[\frac{\Big(q_0 - \xi\omega\Big)\tau}{2}\right]. \tag{40}$$

But, in the limit of sufficiently large $\tau$, one can make use of

$$\lim_{\tau\to\infty} \frac{1}{\pi\Big(q_0 - \xi\omega\Big)} \sin\left[\frac{\Big(q_0 - \xi\omega\Big)\tau}{2}\right] = \delta\Big(q_0 - \xi\omega\Big), \tag{41}$$

to approximate $\Lambda_s^{(1)}(\xi)$ by

$$\Lambda_s^{(1)}(\xi) \cong 2\pi\widetilde{\gamma}_0 \mathfrak{L}'_s \delta\Big(q_0 - \xi\omega\Big). \tag{42}$$

where

$$\mathfrak{L}'_s\Big(\chi_{p_f q_i}, \gamma'_{p_f q_i}\Big) \equiv \exp\Big(-\imath s\chi_{p_f q_i}\Big) J_s\Big(g_0\gamma'_{p_f q_i}\Big) \tag{43}$$

Finally, in order to keep our (approximate) analysis of $S_{rs}^{fi}$ close to that of $S_{r=0,s=0}^{fi}$, we set $b = b' = 0$ and approximate $\mathfrak{F}'_{-r}$ by

$$\mathfrak{F}'_{-r} \cong \hat{\epsilon}^* \mathfrak{L}'_{-r}\Big(\chi_{q_i p_i}, \gamma'_{q_i p_i}\Big)\eta_+(\phi + 1/2)\Big(1 - \eta_+(\phi - 1/2)\Big)$$
$$= \hat{\epsilon}^* \exp\Big(\imath r\chi_{q_i p_i}\Big) J_{-r}\Big(g_0\gamma'_{q_i p_i}\Big)\eta_+(\phi + 1/2)\Big(1 - \eta_+(\ phi - 1/2)\Big). \tag{44}$$

Then,

$$\Lambda_{-r}^{(2)}(\xi) \cong 2\pi\delta\Big(\xi\omega\Big)\hat{\epsilon}^* \mathfrak{L}'_{-r} \tag{45}$$

When Eqs. (42)-(45) are inserted into Eq. (22), one finds that

$$\overline{u}_f B_{rsi} u_i \cong \frac{8\pi^2}{\mid \vec{q} \mid^2} \overline{u}_f \frac{\mathfrak{L}'_s \widetilde{\gamma}_0 (\hat{q}_i + m_0)\hat{\epsilon}^* \mathfrak{L}'_{-r}}{q_i^2 - m_0^2} u_i \delta\Big(q_0\Big). \tag{46}$$

Similarly, one would derive that

$$\overline{u}_f B_{rsf} u_i \cong \frac{8\pi^2}{\mid \vec{q} \mid^2} \overline{u}_f \frac{\mathfrak{L}''_{-r} \hat{\epsilon}^* (\hat{q}_f + m_0)\widetilde{\gamma}_0 \mathfrak{L}''_s}{q_f^2 - m_0^2} u_i \delta\Big(q_0\Big), \tag{47}$$

where $\mathfrak{L}''_s$ and $\mathfrak{L}''_{-r}$ are derived from $\mathfrak{L}'_s$ and $\mathfrak{L}'_{-r}$ by the replacement of $\chi_{p_f q_i}$ and $\gamma'_{p_f q_i}$ by $\chi_{q_f p_i}$ and $\gamma'_{q_f p_i}$.

### C. Resonant denominators

Eqs. (46) and (47) contain two denominators that can be evaluated using the extended semi-classical energy-momentum relationships of Eqs. (9), (10), (16), and (17). From Eq. (9), for example,

$$q_i^2 - m_0^2 \cong 2r(p_i k) - 2(p_i k') - 2r(kk'). \tag{48}$$

Similarly,

$$q_f^2 - m_0^2 \cong -2r(p_f k) + 2(p_f k') + 2r(kk'). \tag{49}$$

In this paper, we are interested in bremsstrahlung emissions that are capable of photoionizing n=2 electrons from the M-shell ions of xenon. The energy range of interest, therefore, is roughly 5.6 keV $\lesssim \omega' \lesssim$ 10 keV, which is to be compared to $E_i > 511$ keV and to $|\vec{p}_i| \sim 200 - 300$ keV. Thus, on defining five angles, $\theta_i$, $\theta_i'$, $\theta_f$, $\theta_f'$, and $\theta$, by

$$(p_i k) \equiv \omega\Big(E_i - |\vec{p}_i|\cos\theta_i\Big), \qquad (p_i k') \equiv \omega'\Big(E_i - |\vec{p}_i|\cos\theta_i' \ Bigr), \tag{50}$$

$$(p_f k) \equiv \omega\Big(E_f - |\vec{p}_f|\cos\theta_f\Big), \qquad (p_f k') \equiv \omega'\Big(E_f - |\vec{p}_f|\cos\theta_i' \ Bigr), \tag{51}$$

and

$$(kk') \equiv \omega\omega'\Big(1 - \cos\theta\Big), \tag{52}$$

one finds that

$$q_i^2 - m_0^2 = 2\omega'|\vec{p}_i|\left(\cos\theta_i' - \cos\theta_i - \frac{\omega'}{|\vec{p}_i|}\Big(1 - \cos\theta\Big)\right), \tag{53}$$

$$q_f^2 - m_0^2 = -2\omega'|\vec{p}_f|\left(\cos\theta_f' - \cos\theta_f - \frac{\omega'}{|\vec{p}_f|}\Big(1 - \cos\theta\Big)\right), \tag{54}$$

when the resonance condition, $\omega' = r\omega$, is satisfied, where

$$\cos\theta = \cos\theta_i'\cos\theta_i + \sin\theta_i'\sin\theta_i\cos\phi_i \tag{55}$$

$$= \cos\theta_f'\cos\theta_f + \sin\theta_f'\sin\theta_f\cos\phi_f. \tag{56}$$

Note that the resonance condition together with Eq. (15) imply that

$$E_f = E_i - s\omega, \tag{57}$$

i.e., when $r\omega$ laser photons are emitted ($r > 0$) as a form of harmonically generated bremsstrahlung, electrons are simultaneously being cooled ($s > 0$) or heated ($s < 0$) by stimulated emission or absorption of $s\omega$ laser photons.

Eqs. (53) and (54) show that the energy denominators of $B_{rsi}$ and $B_{rsf}$ will vanish at a resonance when the bremsstrahlung photon is emitted at an angle, $\theta'_{i,f}$, relative to the initial or final momentum of the electron that is approximately equal to the angle, $\theta_{i,f}$, of the laser beam relative to these momenta. This resonance condition is approximate because of the presence of the $(kk')$ term. Since $\omega'/|\vec{p}_i| = O(1/10)$ is a small quantity, a correction to the resonance at the angles, $\theta_{i,f}$, can be obtained as follows. On substituting Eq. (55) into Eq. (53), an integration over the angles of the bremsstrahlung emission, $d\Omega' = \sin\theta'_i d\theta'_i d\phi_i$, of the energy denominator, $1/(q_i^2 - m_0^2)^2$, and one encounters an integration of the form,

$$I_0 = \int_0^{2\pi} d\phi \, \frac{1}{(a + b\cos\phi)^2} = \frac{2\pi a}{(a^2 + b^2)^{3/2}}, \tag{58}$$

where, for example, $b = (\omega'/|\vec{p}_i|)\sin\theta'_i \sin\theta_i$. Since $b^2 = O((\omega'/|\vec{p}_i|)^2)$, this term can be set to zero yielding $I_0 \cong 2\pi/a^2$, where

$$\begin{aligned} a &= \cos\theta'_i - \cos\theta_i - \frac{\omega'}{|\vec{p}_i|}\Big(1 - \cos\theta_i\cos\theta'_i\Big) \\ &= \left(1 + \frac{\omega'}{|\vec{p}_i|}\cos\theta_i\right)\left\{\cos\theta'_i - \frac{\Big(\cos\theta_i + \omega'/|\vec{p}_i|\Big)}{1 + \Big(\omega'/|\vec{p}_i|\Big)\cos\theta_i}\right\}. \end{aligned} \tag{59}$$

Thus, Eqs.(53) and (54) can be rewritten as

$$q_i^2 - m_0^2 \cong 2\omega'|\vec{p}_i|\left(1 + \frac{\omega'}{|\vec{p}_i|}\cos\theta_i\right)\Big(\cos\theta'_i - \cos\theta_i^{res}\Big), \tag{60}$$

$$q_f^2 - m_0^2 \cong -2\omega'|\vec{p}_f|\left(1 + \frac{\omega'}{|\vec{p}_f|}\cos\theta_f\right)\Big(\cos\theta'_f - \cos\theta_f^{res}\Big), \tag{61}$$

where

$$\cos\theta_i^{res} \equiv \frac{\cos\theta_i + \omega'/|\vec{p}_i|}{1 + \Big(\omega'/|\vec{p}_i|\Big)\cos\theta_i} \tag{62}$$

$$\cos\theta_f^{res} \equiv \frac{\cos\theta_f + \omega'/|\vec{p}_f|}{1 + \Big(\omega'/|\vec{p}_f|\Big)\cos\theta_f}. \tag{63}$$

In the case, therefore, where $\tau \to \infty$, both $B_{rsi}$ and $B_{rsf}$ become infinite at $\theta'_i = \theta_i^{res}$ and at $\theta'_f = \theta_f^{res}$ respectively. For a finite $\tau$, however, we can borrow from Ref.[2] and replace Eqs. (60) and (61) with

$$q_i^2 - m_0^2 \cong 2\omega'|\vec{p}_i|\left(1 + \frac{\omega'}{|\vec{p}_i|}\cos\theta_i\right)\left(\cos\theta'_i - \cos\theta_i^{res} + \imath C_\tau^i\right), \tag{64}$$

$$q_f^2 - m_0^2 \cong -2\omega'|\vec{p}_f|\left(1 + \frac{\omega'}{|\vec{p}_f|}\cos\theta_f\right)\left(\cos\theta'_f - \cos\theta_f^{res} + \imath C_\tau^f\right), \tag{65}$$

where, from Eqs. (72)-(88) of Ref.[2],

$$C_\tau^i = \frac{(kq_i)}{\omega'|\vec{p}_i|}\frac{2}{\sqrt{a_2}\omega\tau}, \tag{66}$$

$$C_\tau^f = \frac{(kq_f)}{\omega'|\vec{p}_f|}\frac{2}{\sqrt{a_2}\omega\tau} \tag{67}$$

and $a_2 \cong 0.5$.

An estimate for the size of $C_\tau^i$ that is of interest to the 2.8 $\mathring{A}$ x-ray lasing experiment can be made as follows. In accord with the experiments of Refs.[7] and in keeping with the photon spectrum[9, 10] needed for the photoionization of n=2 inner-shell electrons, we take for a 50 keV electron, for example, $\hbar\omega = 5$ eV, $\hbar\omega' \geq 5.6$ keV, $m_0c^2 \cong 511$ keV, $|\vec{p}_i|c \sim 240$ keV, $v_i \sim 0.42$, $\omega = 7.6 \times 10^{15}$ s$^{-1}$, and $\tau \cong 250 \times 10^{-15}s$.

$$\begin{aligned}(kq_i) \cong (kp_i) &= \omega\Big(E_i - \hat{n}\cdot\vec{p}_i\Big) \cong \omega\Big(E_i - |\vec{p}_i|\cos\theta_i\Big)\Big|_{\cos\theta_i=1} \\ &= m_0\omega\left(\frac{1-v_i}{\sqrt{1-v_i^2}}\right)\Bigg|_{v_i=0.42} \cong 0.64 m_0\omega.\end{aligned} \tag{68}$$

Therefore, on putting back the $\hbar$'s and $c$'s:

$$C_\tau^i \cong 2\sqrt{2}\times 0.64\left(\frac{\hbar\omega}{\hbar\omega'}\right)\left(\frac{m_0c^2}{|\vec{p}_i|c}\right)\left(\frac{1}{\omega\tau}\right) \sim 1.8\left(\frac{0.9}{10^3}\right)2.1\left(\frac{1}{7.6*250}\right) \sim 2\times 10^{-6}. \tag{69}$$

The smallness of $C_\tau^i$ produces a large amplification factor to the bremsstrahlung emission rate when either $\theta_i' = \theta_i^{res}$ or $\theta_f' = \theta_f^{res}$. Since the laser pulse in the experiments propagates a couple of millimeters in a narrow channel through the gas of xenon clusters, enhanced bremsstrahlung emissions above 5.6 keV within the channel would act to generate L-shell hole states along the way.

## III. THE BREMSSTRAHLUNG CROSS-SECTION IN THE ABSENCE OF AN INTENSE LASER FIELD

In the absence of an external field ($F_0 = 0$), the parameter $\eta_0$ vanishes [Eq. (1)] and thus

$$\gamma_{p_f q_i} = \gamma_{q_i p_i} = \gamma_{p_f q_f} = \gamma_{q_f p_i} = 0, \tag{70}$$

yielding

$$\mathfrak{L}_s' = \mathfrak{L}_s'' = \delta_{s0}, \qquad \mathfrak{L}_{-r}' = \mathfrak{L}_{-r}'' = \delta_{r0}. \tag{71}$$

In this case, Eq. (21) becomes [on substituting Eqs. (71) into Eqs. (46) and (47)]:

$$S_{00}^{fi} = -\imath \frac{Ze^3\sqrt{\pi}}{\sqrt{2\omega' E_f E_i}} \frac{8\pi^2}{|\vec{q}|^2} \overline{u}_f \Big\{ \frac{\widetilde{\gamma}_0\Big((q_i\widetilde{\gamma}) + m_0\Big)(\epsilon^*\widetilde{\gamma})}{q_i^2 - m_0^2} + \frac{(\epsilon^*\widetilde{\gamma})\Big((q_f\widetilde{\gamma}) + m_0\Big)\widetilde{\gamma}_0}{q_f^2 - m_0^2} \Big\} u_i \delta\Big(q_0\Big), \quad (72)$$

where $q_i = p_i - k'$ and $q_f = p_f + k'$ [Eqs. (9) and (16)] and $\delta(q_0) = \delta(\omega' + E_f - E_i)$.

To summarize briefly, the differential cross section, $d\sigma_{fi}$, for radiating a bremsstrahlung photon of frequency, $\omega'$, in the absence of an external (classical) radiation field, is obtained from $|S_{00}^{fi}|^2$ by multiplying in a phase-space-factor and making a flux division[1]:

$$d\sigma_{fi} = \frac{1}{|\vec{v}_i|} \frac{1}{T} \Big|S_{00}^{fi}\Big|^2 \frac{d^3p_f}{(2\pi)^3} \frac{d^3k'}{(2\pi)^3}, \quad (73)$$

where $T$ is an observation time, $T \gtrsim \tau$ and one takes $T = 2\pi\delta(0) = 2\pi\delta(\omega' + E_f - E_i)$[1] to cancel out one of the energy delta functions present in $\Big|S_{00}^{fi}\Big|^2$. Eq. (73) can now be rewritten as

$$d\sigma_{fi} = \frac{Z^2e^6}{|\vec{v}_i|} \frac{(2\pi)^4}{\omega' E_f E_i} \frac{1}{|\vec{q}|^4} \Big|\epsilon^\mu M_\mu(k')\Big|^2 \delta\Big(\omega' + E_f - E_i\Big) \frac{d^3p_f}{(2\pi)^3} \frac{d^3k'}{(2\pi)^3}, \quad (74)$$

where, on use of $q_i^2 - m_0^2 = -2(p_ik')$ and $q_f^2 - m_0^2 = 2(p_fk')$,

$$M_\mu(k') \equiv \overline{u}_f \widehat{M}_\mu(k') u_i \quad (75)$$

and

$$\widehat{M}_\mu(k') \equiv \frac{\widetilde{\gamma}_0\Big((q_i\widetilde{\gamma}) + m_0\Big)\widetilde{\gamma}_\mu}{2(p_ik')} - \frac{\widetilde{\gamma}_\mu\Big((q_f\widetilde{\gamma}) + m_0\Big)\widetilde{\gamma}_0}{2(p_fk')}. \quad (76)$$

A cross section for unpolarized bremsstrahlung production from the scattering of unpolarized electrons can now be obtained from $d\sigma_{fi}$ by summing over polarizations and by summing and averaging over spins:

$$d\langle\sigma\rangle^{fi} = \frac{Z^2e^6}{|\vec{v}_i|} \frac{(2\pi)^4}{\omega' E_f E_i} \frac{F}{|\vec{q}|^4} \delta\Big(\omega' + E_f - E_i\Big) \frac{d^3p_f}{(2\pi)^3} \frac{d^3k'}{(2\pi)^3}, \quad (77)$$

where

$$\begin{aligned} F &\equiv \frac{1}{2} \sum_{\lambda'=1}^{2} \sum_{s_i, s_f} \Big|\epsilon^\mu(k', \lambda') \overline{u}_f(s_f) \widehat{M}_\mu u_i(s_i)\Big|^2 \\ &= \frac{1}{2} \sum_{\lambda'=1}^{2} \epsilon_\mu(k', \lambda') \epsilon_\nu^*(k', \lambda') Tr\Big\{ \widehat{M}^\mu\Big((p_i\widetilde{\gamma}) + m_0\Big) \widehat{M}^{\nu+}\Big((p_f\widetilde{\gamma}) + m_0\Big)\Big\}. \end{aligned} \quad (78)$$

By substituting

$$d^3p_f = |\vec{p}_f| E_f d\Omega_f dE_f, \qquad d^3k' = \omega'^2 d\Omega' d\omega', \quad (79)$$

and by noting that the initial electron velocity, $|\vec{v_i}|$, is given by $|\vec{v_i}| = |\vec{p_i}|/E_i$, one can then carry out the $E_f$ integration to write the bremsstrahlung cross section in the form,

$$\frac{d\langle\sigma\rangle^{fi}}{d\Omega' d\omega' d\Omega_f} = \frac{|\vec{p}_f|}{|\vec{p_i}|}\frac{Z^2e^6\omega' F}{|\vec{q}|^4}\frac{1}{(2\pi)^2}\eta_+(E_i - m_0 - \omega'). \tag{80}$$

Because Eq. (76) implies that $k'_\mu \widehat{M}^\mu = 0$, one can rewrite $F$ in a relativistically invariant form as

$$F = -\frac{1}{2}Tr\Big\{\widehat{M}^\mu\Big((p_i\widetilde{\gamma}) + m_0\Big)\widehat{M}^+_\mu\Big((p_f\widetilde{\gamma}) + m_0\Big)\Big\}. \tag{81}$$

Since $\widehat{M}_\mu$ is made of two terms, $F$ has four terms, which are denoted here using the same notation as is found in Ref.[1] but with a different spinor normalization:

$$F = -\frac{1}{8}\Big\{\frac{1}{(p_fk')^2}F_1 + \frac{1}{(p_ik')^2}F_2 - \frac{1}{(p_ik')(p_fk')}\Big(F_3 + F_4\Big)\Big\}, \tag{82}$$

As in Ref.[2], we are interested only in estimating the relative sizes of the bremsstrahlung cross sections in the absence of and in the presence of an intense laser field. Given that each of the four $F_i$, $i = 1, \cdots, 4$ terms make comparable contributions to these cross sections, and, as in Ref. [2], for algebraic simplicity, we focus here only on the $F_2$ term in $F$ and ratio only the part of the two cross sections that contain this term, which is given by

$$F_2 = Tr\Big\{\widetilde{\gamma}_0\Big((q_i\widetilde{\gamma}) + m_0\Big)\widetilde{\gamma}_\mu\Big((p_i\widetilde{\gamma}) + m_0\Big)\widetilde{\gamma}^\mu\Big((q_i\widetilde{\gamma}) + m_0\Big)\widetilde{\gamma}_0\Big((p_f\widetilde{\gamma}) + m_0\Big)\Big\}, \tag{83}$$

Again, from Ref.[1], in the absence of a laser field,

$$\begin{aligned} F_2 &= 16\Big\{m_0^4 + m_0^2\Big((\tilde{p}_ip_f) - (\tilde{p}_fk') - (p_ik')\Big) - (p_ik')(\tilde{p}_fk')\Big\} \\ &= 16\Big\{m_0^4 + m_0^2\Big((\tilde{p}_ip_f) - \omega'\Big[(n'\tilde{p}_f) - (n'p_i)\Big]\Big) - \omega'^2(n'p_i)(n'\tilde{p}_f)\Big\}, \end{aligned} \tag{84}$$

where $\tilde{p}_{i,f} \equiv (E_{i,f}, -\vec{p}_{i,f})$. For the problem of interest, $E_i$ and $E_f \sim 560$ keV, $|\vec{p}_i|$ and $|\vec{p}_f| \sim 250$ keV, and $\omega' \sim 6$ keV. Thus, one can rewrite Eq. (84) as $F_2 = 16\Big(m_0^4 + m_0^2(\tilde{p}_ip_f)\Big) +$ (lower order terms), and approximate $F_2$ by $F_2 \cong 16\Big(m_0^4 + m_0^2(\tilde{p}_ip_f)\Big)$. On writing $d\langle\sigma\rangle^{fi} = \sum_{n=1}^4 d\langle\sigma_n\rangle^{fi}(F_n)$ and on using $(p_ik') = \omega'(E_i - |\vec{p}_i|\cos\theta'_i)$, one then finds that

$$\begin{aligned} \frac{d\langle\sigma_2\rangle^{fi}}{d\omega' d\Omega_f} &\sim -\frac{|\vec{p}_f|}{|\vec{p_i}|}\Big(m_0^4 + m_0^2(\tilde{p}_ip_f)\Big)\frac{Z^2e^6\omega'}{|\vec{q}|^4}\frac{1}{2\pi^2}\eta_+(E_f - m_0) \times \\ &\qquad \int_0^\pi \sin\theta'_i d\theta'_i \int_0^{2\pi} d\phi_i \frac{1}{\omega'^2(E_i - |\vec{p_i}|\cos\theta'_i)^2} \\ &= -\frac{2}{\pi}\Big(m_0^2 + (\tilde{p}_ip_f)\Big)\frac{|\vec{p}_f|}{|\vec{p_i}|}\frac{Z^2e^6}{\omega'}\frac{1}{|\vec{q}|^4}\eta_+(E_i - m_0 - \omega'). \end{aligned} \tag{85}$$

## IV. THE BREMSSTRAHLUNG CROSS-SECTION IN THE PRESENCE OF AN INTENSE LASER FIELD

### A. Semi-classical cross section

Because the theory being used to calculate a bremsstrahlung cross section in the presence of an intense laser field is part quantum electrodynamic and part classical, it inherently does not allow the computation of a bremsstrahlung cross section from a given initial laser photon number state, $|N\rangle$ to a final laser photon number state$|N+s-r\rangle$ ($s-r<0$ or $s-r>0$). However, as was done in Ref. [2], we take the semi-classical definition of such a cross section to be the following generalization of Eq. (73):

$$d\sigma_{rs}^{fi}=\frac{1}{|\vec{v}_i|}\frac{1}{T}\Big|S_{rs}^{fi}\Big|^2\frac{d^3p_f}{(2\pi)^3}\frac{d^3k'}{(2\pi)^3}, \tag{86}$$

In this case, the peak in laser intensity is given by $I_{\ell aser}^{max}=F_0^2/(8\pi)=N\omega/V$, where V is the laser field's quantization volume.

The dimensionless coupling strength, $\eta_0$, given by Eq. (2), lies between values of 0.67 and 2.12 for strong laser fields for which, $10^{19}\leq I_{\ell aser}\leq 10^{20}$ W/cm$^2$, $\eta_0$ and is, thus, not a good expansion parameter. In this case, the substitution of Eq. (43) replaces that of Eqs. (71) in Eq. (46). Note that, in general, there are two parts to $\mathfrak{F}'_{-r}$ producing two parts to $\overline{u}_f B_{rsi}u_i$. However, in order to make a simplified comparison of bremsstrahlung formulas, with and without the presence of an intense laser field, we shall set aside, as noted earlier, the $b_0$ contributions to $\overline{u}_f B_{rsi}u_i$, and analyze only the $F_2$ contribution to it, which comes from the $S_{rsi}$ part of $S_{rs}^{fi}=S_{rsi}+S_{rsf}$:

$$\begin{aligned}S_{rsi}=-\imath\frac{Ze^3\sqrt{\pi}}{\sqrt{2\omega' E_f E_i}}\frac{8\pi^2}{|\vec{q}|^2}\overline{u}_f\left\{\frac{\widetilde{\gamma}_0\Big((q_i\widetilde{\gamma})+m_0\Big)(\epsilon^*\widetilde{\gamma})}{q_i^2-m_0^2}\right\}u_i\times\\ \exp\Big(-\imath s\chi_{p_f q_i}\Big)J_s\Big(g_0\gamma'_{p_f q_i}\Big)\exp\Big(\imath r\chi_{q_i p_i}\Big)J_{-r}\Big(g_0\gamma'_{q_i p_i}\Big)\delta\Big(q_0\Big),\end{aligned} \tag{87}$$

Thus, because $q_i^2-m_0^2\cong 2\omega'|\vec{p}_i|\Big(\cos\theta'_i-\cos\theta_i+\imath C_r^i\Big)$ [Eq. (64)],

$$\begin{aligned}d\sigma_{2rs}^{fi}&=\frac{1}{|\vec{v}_i|}\frac{1}{T}\Big|S_{rsi}\Big|^2\frac{d^3p_f}{(2\pi)^3}\frac{d^3k'}{(2\pi)^3}\\ &=\frac{Z^2e^6}{|\vec{v}_i|}\frac{1}{\omega' E_f E_i}\frac{(2\pi)^4}{|\vec{q}|^4}\Big|\epsilon^\mu M_\mu^{(2)}(k')\Big|^2\Big|J_s\Big(g_0\gamma'_{p_f q_i}\Big)\Big|^2\Big|J_{-r}\Big(g_0\gamma'_{q_i p_i}\Big)\Big|^2\\ &\cdot\ \delta\Big(\omega'+E_f-E_i+(s-r)\omega\Big)\frac{|\vec{p}_f|E_f d\Omega_f dE_f}{(2\pi)^3}\frac{\omega'^2 d\Omega' d\omega'}{(2\pi)^3},\end{aligned} \tag{88}$$

where

$$M_\mu^{(2)}(k') = \overline{u}_f \widehat{M_{r\mu}}^{(2)}(k') u_i. \tag{89}$$

and

$$\widehat{M_{r\mu}}^{(2)}(k') \equiv \left. \frac{\widetilde{\gamma}_0\Big((q_i\widetilde{\gamma}) + m_0\Big)\widetilde{\gamma}_\mu}{2\omega'|\vec{p}_i|\Big(\cos\theta_i' - \cos\theta_i^{res} + \imath C_r^i\Big)} \right|_{q_i = p_i - k' + rk}. \tag{90}$$

As before, one next needs to sum and average $\left|\epsilon^\mu M_\mu^{(2)}(k')\right|^2$ over spins as well as to sum over polarizations. One then obtains

$$\begin{aligned}
&\frac{1}{2}\sum_{\lambda'=1}^{2}\sum_{s_i,s_f}\left|\epsilon^\mu(k',\lambda')\overline{u}_f(s_f)\widehat{M}_\mu^{(2)}u_i(s_i)\right|^2 \\
&\quad\cong -\frac{1}{8}\frac{Tr\Big\{\widetilde{\gamma}_0\Big((q_i\widetilde{\gamma}) + m_0\Big)\widetilde{\gamma}_\mu\Big((p_i\widetilde{\gamma}) + m_0\Big)\widetilde{\gamma}^\mu\Big((q_i\widetilde{\gamma}) + m_0\Big)\widetilde{\gamma}_0\Big((p_f\widetilde{\gamma}) + m_0\Big)\Big\}}{\omega'^2|\vec{p}_i|^2\Big\{(\cos\theta_i' - \cos\theta_i^{res})^2 + C_r^{i2}\Big\}} \\
&\quad\equiv -\frac{1}{8}\frac{F_{2r}}{\omega'^2|\vec{p}_i|^2\Big\{(\cos\theta_i' - \cos\theta_i^{res})^2 + (C_r^i)^2\Big\}},
\end{aligned} \tag{91}$$

Finally, on inserting Eq. (91) into Eq. (89) and on integrating the resulting equation over $E_f$, one obtains

$$\begin{aligned}
\frac{d\langle\sigma_2\rangle_{rs}^{fi}}{d\Omega' d\omega' d\Omega_f} = &-\frac{|\vec{p}_f|}{32\pi^2\omega'|\vec{p}_i|^3}\frac{Z^2e^6F_{2r}}{|\vec{q}|^4}\Big|J_s\Big(g_0\gamma'_{p_fq_i}\Big)\Big|^2\Big|J_{-r}\Big(g_0\gamma'_{q_ip_i}\Big)\Big|^2 \\
&\cdot\frac{1}{\Big(\cos\theta_i' - \cos\theta_i^{res}\Big)^2 + (C_r^i)^2}\eta_+\Big(E_i - \omega' - (s-r)\omega - m_0\Big).
\end{aligned} \tag{92}$$

We note, because of $q_i$'s dependence on $rk$, that $F_2$ is modified from its value given in Eq. (84). The (small) correction terms to it as well as those for $F_1$, $F_3$, and $F_4$ are given in Appendix I. Note further, as before, that had the $b_0$ term been kept, there would be a trace over eight, rather than four, gamma matrices to be evaluated. On following the procedures for evaluating such traces, which are described in Ref. [1], one would derive an expression containing 105 terms. Such a calculation is beyond the purview of this paper.

### B. Bessel function analysis

Eqs. (91) and (92) add several correction terms to Eq.(80). One, a non-resonant denominator has been replaced by a resonant one. Two, the $F_2$ factor has been replaced by $F_{r2}$. Three, in the scattering of an electron from an ion, the final electron energy, $E_f$, now equals the initial energy of the electron minus the radiation energy emitted as bremsstrahlung and

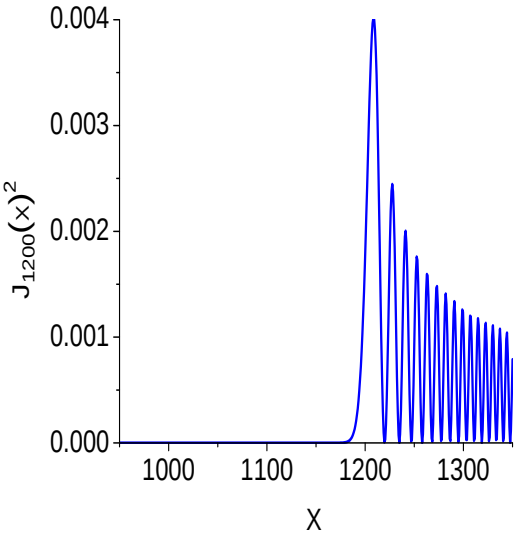


FIG. 3. The Bessel function, $J_{1200}$, squared is shown as a function of its argument, $x$, in a region surrounding the value of its index, 1200. Nonzero values of significance are reached only for $x \gtrsim 1200$.

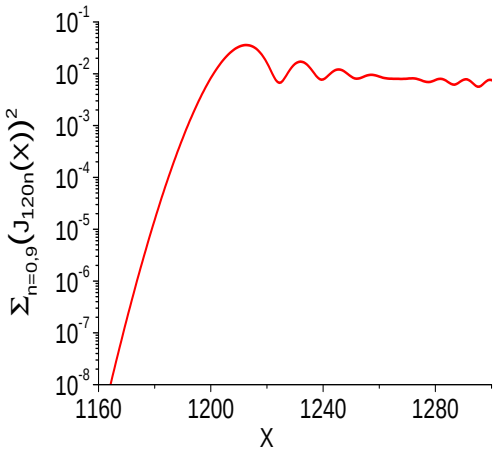


FIG. 4. A sum over Bessel functions squared from $J^2_{1200}$ to $J^2_{1209}$ is shown for values of the argument just below the Bessel function index to values well beyond. Oscillations are still present, but they no longer go to zero as in Fig. 3.

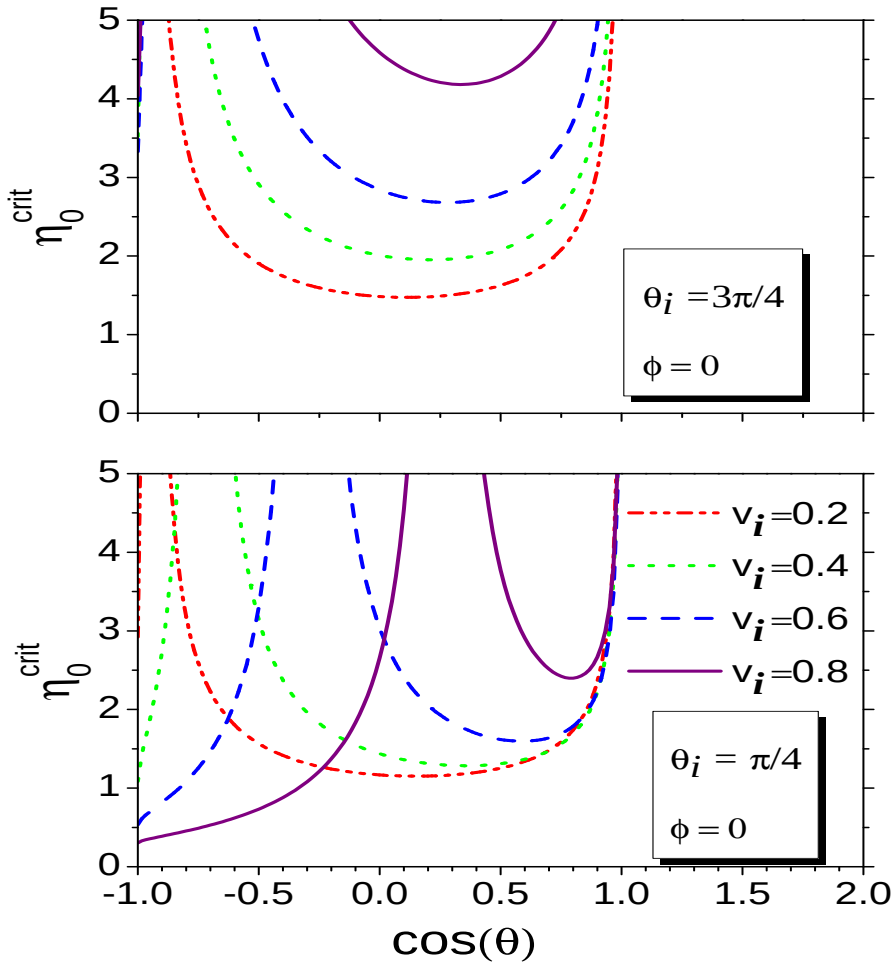


FIG. 5. Plots of $\eta_0^{crit}$ as a function of the cosine of the angle between the laser beam and the propagation direction of the bremsstrahlung photons are shown for four different electron velocities, $v_i$, and for $\phi = 0$. Two cases involving different angles of the bremsstrahlung emission with respect to the incident momentum of the scattered electron are compared.

plus or minus any energy gained or lost to the laser field. And four, the strength by which $r + s$ laser photons are emitted or absorbed is tempered by the presence of the two Bessel functions, whose strengths are determined by the magnitudes of their arguments, $g_0\gamma'_{p_f q_i}$ and $g_0\gamma'_{q_i p_i}$ [see Figs. 3 and 4].

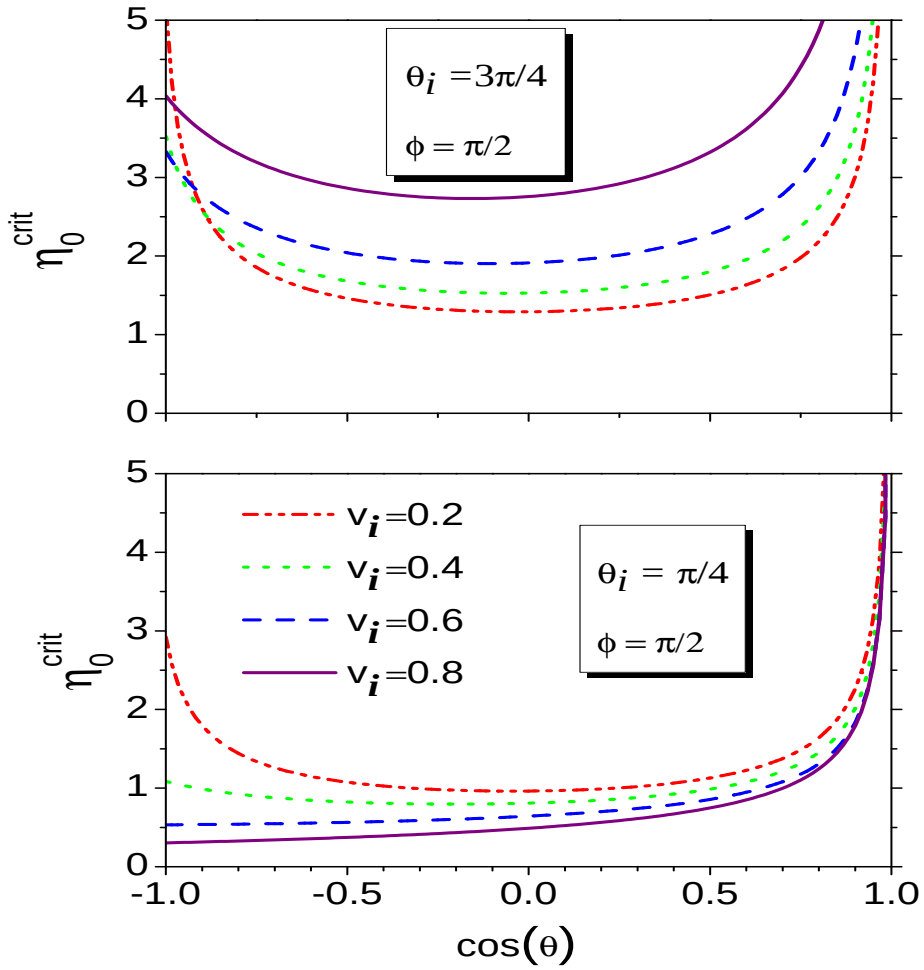


FIG. 6. Plots of $\eta_0^{crit}$ as a function of the cosine of the angle between the laser beam and the propagation direction of the bremsstrahlung photons are shown for four different electron velocities, $v_i$, and for $\phi = \pi/2$. Two cases involving different angles of the bremsstrahlung emission with respect to the incident momentum of the scattered electron are compared.

The definitions of $\gamma'_{p_f q_i}$ and $\gamma'_{q_i p_i}$ are given in Eqs. (35) and (36). These expressions can be rewritten using $k = \omega(1, 0, 0, 1)$, which implies

$$(kQ_{q_i,p_i}) = \omega\{Q^0_{q_i,p_i} - Q^3_{q_i,p_i}\} = 0, \quad \rightarrow \quad Q^0_{q_i,p_i} = Q^3_{q_i,p_i}. \tag{93}$$

Thus, $(e_x Q)^2 + (e_y Q)^2 = (Q^1_{q_i p_i})^2 + (Q^2_{q_i p_i})^2 + (Q^3_{q_i p_i})^2 - (Q^0_{q_i p_i})^2 = -(Q_{q_i p_i} Q_{q_i p_i})$ and, from

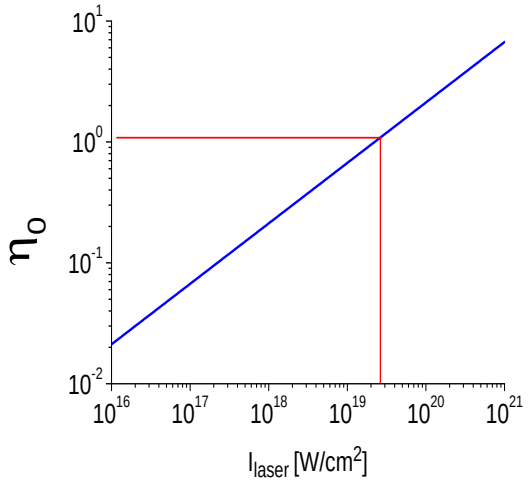


FIG. 7. $\eta_0$ as a function of laser intensity, $I_{laser}$.

Eqs. (37),

$$\begin{aligned}\gamma_{q_ip_i} &= g_0\eta_0 m_0\sqrt{-(Q_{q_ip_i}Q_{q_ip_i})} \\ &= \frac{g_0\eta_0 m_0}{(kp_i)(kq_i)}\sqrt{2(p_iq_i)(kp_i)(kq_i)-(q_iq_i)(kp_i)^2-(p_ip_i)(kq_i)^2}. \end{aligned} \tag{94}$$

Finally, because $(kq_i) = (kp_i) - (k'k)$, $(q_iq_i) = m_0^2 - 2(k'p_i) + 2r(kp_i) - 2r(k'k)$, and $(p_iq_i) = m_0^2 - (k'p_i) + r(kp_i)$ and since $\omega' = r\omega$, one then finds that

$$g_0\gamma'_{q_ip_i} = \eta_0\frac{g_0m_0\,r}{(np_i)(nq_i)}\sqrt{(n'n)\Big\{2(n'p_i)(np_i) - m_0^2(n'n)\Big\}} \equiv a_{q_ip_i}\eta_0\,r. \tag{95}$$

Note, when $\eta_0 = 1/a_{q_ip_i} \equiv \eta_0^{crit}$, that $\gamma_{q_ip_i} = r$ and $J_r(g_0\gamma'_{q_ip_i}) = J_r(r)$. Figs. 3 and 4 show $r$ to be close to the argument of the Bessel function, $J_r$, at which it reaches its highest value.

The 4-vector products in Eq. (95) involve the angles, $\theta_i$ and $\theta'_i$, defined in Eqs. (50) as well as an angle, $\theta$, defined in Eq. (52) as the direction of the laser photon relative to the bremsstrahlung photon:

$$(nn') = 1 - \cos\theta. \tag{96}$$

The angles between the three vectors, $\hat{n}$, $\hat{n}'$, and $\vec{p}_i$, are related by $\cos\theta'_i = \cos\theta_i\cos\theta + \sin\theta_i\sin\theta\cos\phi$. Moreover, $(nq_i) = (np_i) - \omega'(nn') = E_i - |\vec{p}_i\cos\theta_i| - \omega'(1-\cos\theta)$. Thus, we can take the three independent angular dependences in Eq. (95) to be $\theta$, $\theta_i$, and $\phi$. Figs. 5 and 6 show how $\eta_0^{crit}$ varies for a variety of bremsstrahlung scatterings for an r value of 1200,

in which $\omega' = r\omega \approx 6$ keV. In these figures, the angle, $\theta$, is varied between 0 and $\pi$ for two values of $\theta_i$, two of $\phi$, and four values of the electron velocity. Values of $\eta_0$ are then shown in Fig. 7 as a function of $I_{laser}^{max}$. Together, Figs. 5-7 show that $\eta_0$ both reached and exceeded critical values in a large variety of scattering angles and throughout the energy spectrum of the electrons in the experiments of Ref. [7].

A similar analysis carried out for $\gamma_{p_f,q_i}$ begins, as above, from Eqs. (35) and (37):

$$\begin{aligned} g_0\gamma'_{p_fq_i} &= g_0\eta_0 m_0\sqrt{-(Q_{p_fq_i}Q_{p_fq_i})} \\ &= \frac{g_0\eta_0 m_0}{\omega(nq_i)(np_f)}\sqrt{2(p_fq_i)(nq_i)(np_f) - (q_iq_i)(np_f)^2 - m_0^2(nq_i)^2}. \end{aligned} \tag{97}$$

and ends, using $q_i = p_f - q + sk$, with

$$g_0\gamma'_{p_f,q_i} = \frac{g_0\eta_0 m_0}{\omega(nq_i)(np_f)}\sqrt{2(p_fq)(nq)(np_f) - (qq)(np_f)^2 - m_0^2(nq)^2}. \tag{98}$$

Thus, the magnitude of $\gamma_{p_f,q_i}$ can be estimated as follows. All terms under the square root are of order $(m_0|\vec{q}|)^2$. Therefore, since $\vec{q} \sim m_0\vec{v}_{i,f}$ and $m_0/(nq_i) = O(1)$, one has that

$$\gamma'_{p_f,q_i} = O\left(\frac{\eta_0|\vec{q}|}{\omega}\right) \sim O\left(\frac{\eta_0 m_0 v_i}{\omega}\right) = O\big(\gamma_0\big). \tag{99}$$

The size of $\gamma_0$ [see Eqs. (1)] varies with $\eta_0$ and $v_i$, but for $\eta_0 \sim 1$ and for a 50 keV electron for which $v_i \sim 1.36 \times 10^{10}$ cm/s, one finds that $\gamma'_{p_f,q_i} \sim m_0 v_i/\omega \sim 10^4$.

### C. $F_2$ enhancement factor

In order to compute a bremsstrahlung-like, harmonic generation rate for $\omega' \cong r\omega$ that is independent of the laser heating or cooling rate of the electrons, one must sum Eq. (92) over all $s$ values:

$$\begin{aligned} \frac{d\langle\sigma_2\rangle_r^{fi}}{d\Omega' d\omega' d\Omega_f} \equiv \sum_{s=-\infty}^{\infty}\frac{d\langle\sigma_2\rangle_{rs}^{fi}}{d\Omega' d\omega' d\Omega_f} \cong -\frac{|\vec{p}_f|}{32\pi^2\omega'|\vec{p}_i|^3}\frac{Z^2e^6F_{r2}}{|\vec{q}|^4}\Big|J_{-r}\Big(g_0\gamma'_{q_ip_i}\Big)\Big|^2 \\ \cdot\frac{1}{\Big(\cos\theta'_i - \cos\theta_i^{res}\Big)^2 + C_r^{i2}}\sum_{s=-\infty}^{\infty}\eta_+\Big(E_i - m_0 - s\omega\Big)\Big|J_s\Big(g_0\gamma'_{p_fq_i}\Big)\Big|^2. \end{aligned} \tag{100}$$

In the problem we are considering, $E_i - m_0$ lies in the tens of kilovolts range, while $\omega \sim 6$ eV; thus $s \sim 10^4$. Using the Bessel function identity, $\sum_{s=-\infty}^{\infty}\Big|J_s\Big(\gamma_{p_fq_i}\Big)\Big|^2 = 1$, one has that

$$\sum_{s=-\infty}^{\infty}\eta_+\Big(E_i - m_0 - s\omega\Big)\Big|J_s\Big(g_0\gamma'_{p_fq_i}\Big)\Big|^2 = 1 - \sum_{s=(E_i-m_0)/\omega}^{\infty}\Big|J_s\Big(g_0\gamma'_{p_fq_i}\Big)\Big|^2 \equiv \alpha. \tag{101}$$

Again, because $E_i > |\vec{p}_i| >> \omega'$ for a 50 keV electron and a 6 keV bremsstrahlung photon, one has that $\alpha \cong 1/2$. Therefore, on setting $F_{r2} \cong F_2 \cong 16\Big(m_0^4 + m_0^2(\tilde{p}_i p_f)\Big)$,

$$\frac{d\langle\sigma_2\rangle_r^{fi}}{d\omega' d\Omega_f} \cong -\frac{|\vec{p}_f|\Big(m_0^4 + m_0^2(\tilde{p}_i p_f)\Big)}{\pi\omega'|\vec{p}_i|^3}\frac{Z^2e^6\alpha}{|\vec{q}|^4}\Big|J_r\Big(g_0\gamma'_{q_i p_i}\Big)\Big|^2\int_0^\pi \frac{\sin\theta' d\theta'}{\Big(\cos\theta'_i - \cos\theta_i^{res}\Big)^2 + C_r^{i2}} \quad (102)$$

and since for very small $C_r^i$,

$$\int_0^\pi \frac{\sin\theta'_i d\theta'_i}{\Big(\cos\theta'_i - \cos\theta_i^{res}\Big)^2 + C_r^{i2}} = \frac{1}{C_r^i}\left\{\arctan\left(\frac{1+\cos\theta_i^{res}}{C_r^i}\right) + \arctan\left(\frac{1-\cos\theta_i^{res}}{C_r^i}\right)\right\}$$
$$\cong \frac{\pi}{C_r^i}, \quad (103)$$

one has that

$$\frac{d\langle\sigma_2\rangle_r^{fi}}{d\omega' d\Omega_f} \cong -\frac{|\vec{p}_f|\Big(m_0^4 + m_0^2(\tilde{p}_i p_f)\Big)}{\omega'|\vec{p}_i|^3}\frac{Z^2e^6}{|\vec{q}|^4}\frac{\alpha}{C_r^i}\Big|J_r\Big(g_0\gamma'_{q_i p_i}\Big)\Big|^2 \quad (104)$$

Finally, from Eqs. (85) and (104), and for $\omega' < E_i - m_0$, one obtains the following enhancement factor, $\eta_2$, derived from the $F_{2r}$ part of the bremsstrahlung emission cross section in the presence of a high intensity laser field:

$$\eta_2 \equiv \frac{d\langle\sigma_2\rangle_r^{fi}}{d\omega' d\Omega_f}\Bigg/\frac{d\langle\sigma_2\rangle^{fi}}{d\omega' d\Omega_f} = \frac{\pi}{2}\frac{m_0^2}{|\vec{p}_i|^2}\Big|J_r\Big(g_0\gamma'_{q_i p_i}\Big)\Big|^2\frac{\alpha}{C_r^i}. \quad (105)$$

Using Eq. (66) (with $\alpha \cong 1/2$ and $a_0 \cong 1/2$), one estimates an enhanced bremsstrahlung emission that is given by

$$\eta_2 \cong \frac{\pi}{8\sqrt{2}}\frac{m_0^2}{|\vec{p}_i|^2}\Big|J_r\Big(g_0\gamma'_{q_i p_i}\Big)\Big|^2\frac{|\mathbf{p}_i|}{(nq_i)}(\omega'\tau). \quad (106)$$

In the Refs. [7] xenon cluster experiments, the laser pulsewidth was $\tau \sim 2.5\times10^{-13}$ s while the bremstrahlung emissions of interest lie above 5.6 keV. In this case, $\omega' \geq 8.5\times10^{18}$ s$^{-1}$ and $\omega'\tau \gtrsim 2.1\times10^6$. Moreover, for a 50 keV electron for which $E_i \cong 560$ keV and $|\vec{p}_i| \cong 240$ keV, $|\vec{p}_i|/(nq_i) \cong |\vec{p}_i|/(E_i - |\vec{p}_i|\cos\theta_i) \cong 1/2$ and from Figs. 3 and 4, $(m_0^2/|\vec{p}_i|^2)\Big|J_r\Big(g_0\gamma'_{q_i p_i}\Big)\Big|^2 \cong 1.6\times10^{-2}$. Therefore, the estimated enhancement is

$$\eta_2 \approx 0.28\times1.6\times10^{-2}\times0.5(\omega'\tau) \approx 4.5\times10^3. \quad (107)$$

## V. COMPARING TO EXPERIMENT: XENON PHOTOIONIZATION ABSORPTION RATES

In their paper on resonant spontaneous bremsstrahlung emission[2], Lebed and Roshchupkin conclude with the statement that their "obtained results may be experimentally verified,

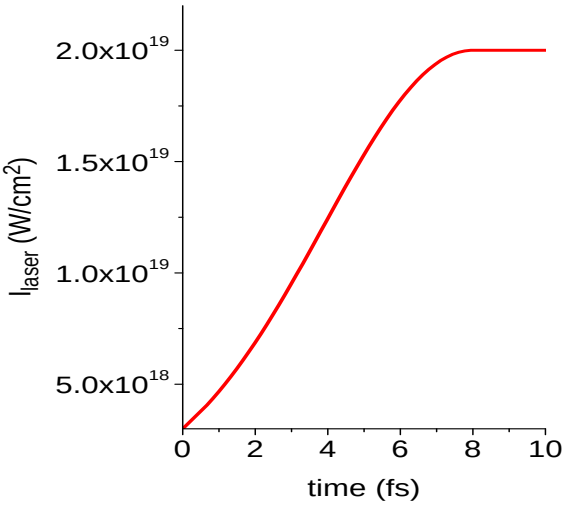


FIG. 8. Laser intensity as a function of time used in the gain calculation that follows.

for example, by the scientific facilities at the SLAC laboratory"; in other words, the theoretical prediction of enhanced bremsstrahlung emission that they had made needs experimental confirmation. The extensions of their work that were made in this paper similarly need to be confirmed.

In this section, we present results from a model calculation that offer indirect support for the above predicted bremsstrahlung enhancement. The experiments that were modeled are described in Ref. [7] and in the references cited therein. In these experiments, KrF laser radiation was focused to intensities greater than $10^{19}$ W/cm$^2$ in a gas of xenon clusters. A prominant double humped collection of n=3 to n=2 radiative transitions, originating from within the various M-shell ionization stages, was observed. Amplified x-ray emissions at $\sim 2.8\mathring{A}$ were also seen within this collection of lines. Moreover, $\eta_0$ values $\gtrsim 1$ were attained in these experiments, and thus, conditions were suitable for the production of enhanced bremsstrahlung as described and predicted above. When they occur at laser photon harmonics greater than 1120, these emissions have sufficient energies, $\geq 5.6$ keV, to begin photoionization of n=2 inner-shell electrons from within the xenon M-shell ionization stages. However, the strength of such emissions has yet to be measured.

A theoretical model of a xenon cluster's early-time dynamics was recently constructed[8–10] in an effort to determine the mechanism by which such n=3 to n=2 x-ray amplifica-

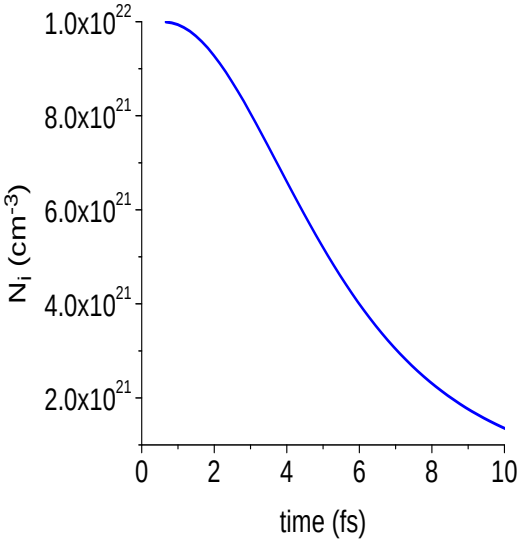


FIG. 9. Average xenon ion density declines rapidly as a function of time

tions could be generated. In this model, a molecular dynamics calculation of the cluster's early-time expansion and heating was combined with a detailed description of the cluster's ionization dynamics both in response to the same intense laser field. A basic assumption made in this modeling was that hole states were generated preferentially by photoionization. The rates of photoionization were determined by the requirement that the calculated gain coefficients matched up with the measured ones. These calculations showed that large photoionization rates were needed in order to theoretically replicate the measured gains. These rates, in turn, produce large power inputs to the xenon ions. In this section, a calculation of this power input is presented and compared to an enhanced Bethe-Heitler bremsstrahlung power output. It is found that enhanced bremsstrahlung emission, if present in the experiments, is of sufficient strength to be the driver of the inner-shell ionizations that are needed to produce the x-ray amplifications seen in the Ref. [7] experiments.

The model calculation is carried out as follows. To begin, a prescribed, time evolving laser intensity is used in the molecular dynamics calculation to obtain average electron and ion densities, $n_e(t)$ and $n_i(t)$, and average effective electron and ion temperatures, $T_e(t)$ and $T_i(t)$, as functions of time. These values are stored and used as input to an ionization dynamics calculation whose rate equations and gain coefficients depend on them. Ground and excited state ion densities are calculated from the ionization dynamics model, and

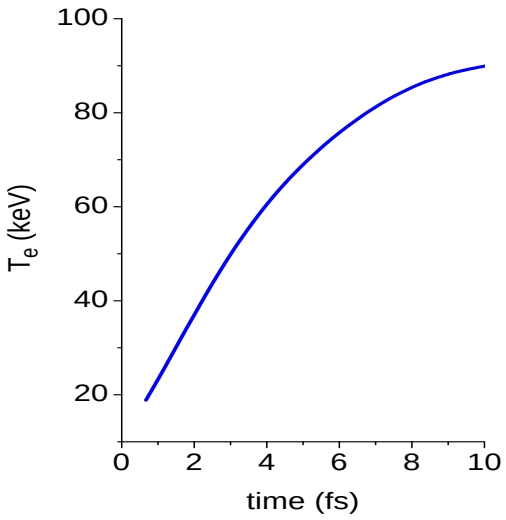


FIG. 10. Effective electron temperature as inferred from the calculated non-Maxwellian electron distribution as a function of time.

fractional populations, $f_\mu(t)$, are thus determined as a function of time. Three essential features built into the rate equation dynamics are (1) tunneling ionization rates are included as part of the dynamics of each ground and valence excited state, (2) there is no charge neutrality in the calculations, i.e., $n_e(t) \neq \sum_\mu Z_\mu f_\mu(t) n_i(t)$, and (3) both single and double hole states are coupled self-consistently into the rate equations. In these calculations, hole states are created by photoionization, at rates that are approximately determned by the strength of the photoionization cross sections, and they are shaped approximately by Bethe-Heitler bremsstrahlung emission rates, which are proportional to $T_e(t) n_i(t)^2$.

A typical calculation is illustrated in Figs. 8-14. Figure 8 shows the rise in laser intensity used to drive the energy absorption, heating, and expansion of a xenon cluster consisting of 200 atoms. In the calculation, a peak intensity of $2 \times 10^{19}$ W/cm$^2$ is reached in 8 fs beginning from an initial intensity of $3 \times 10^{18}$ W/cm$^2$. A fast rise in intensity from this initial value completes the rapid tunnel ionization of a xenon atom through the N-shell, bringing almost the entire cluster into the ground state of the Ni-like xenon ionization stage. In response to the Fig. 8 rise in laser intensity, the cluster Coulomb explodes. Electrons are driven from the cluster, and it rapidly expands (Fig. 9). Electrons undergo a rapid non-equilibrium rise in energy, producing an effective rising temperature (Fig. 10), i.e., the electron distribution

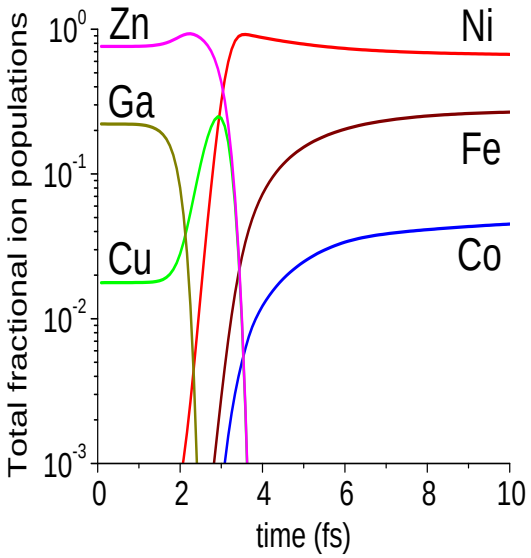


FIG. 11. Total fractional populations, exclusive of hole states, of the Ga-, Zn-, Cu-, Ni-, Co-, and Fe-like ionization stages as a function of time.

function generated in the molecular dynamics calculation is highly non-Maxwellian.

The calculated response of the ion populations to this rise in laser intensity, and to the cluster's heating and expansion, is shown in Fig. 11. Once intensity values greater than $10^{19}$ W/cm$^2$ are reached, effectively all of the xenon ions have been stripped of their N-shell electrons (Fig. 11). At this point in the dynamics and somewhat thereafter, the cluster consists predominantly of Ni-like ions in their ground state. The photoionization of n=2 electrons, which is driven by enhanced bremsstrahlung emissions, can now take place into the $2p_{3/2}$, $2p_{1/2}$, and $2s_{1/2}$ hole states of Co-like xenon. The magnitudes of the rates that are used in this calculation to inner-shell ionize the ground state of Ni-like xenon into these states is shown in Fig. 12. Their relative magnitudes reflect the relative strength of the photoionization cross sections as well as the different energy thresholds, which, for the $2p_{3/2}$, $2p_{1/2}$, and $2s_{1/2}$ states, are 5653, 5975, and 6322 eV respectively in our calculations. These ionization rates are shaped in time by a $T_e(t)^{1/2} n_i(t)^2$ time dependence taken from the bremsstrahlung emissions, but the peak value of $\sim 10^{14}$ s$^{-1}$ of the $2p_{3/2}$ photoionization rate was specifically chosen to produce the calculated gain curves shown in Fig. 13. Given a dilution factor of roughly 1/10 or more due to the gaseous structure of the cluster gain medium, these gain coefficients compare favorably with the ones that were measured.

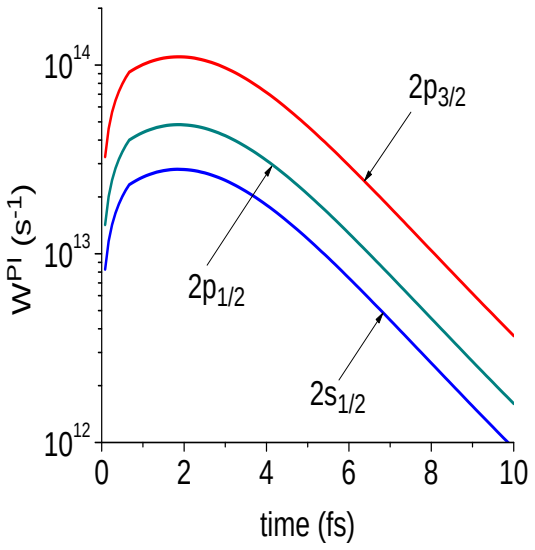


FIG. 12. The photoionization pumping rates of the three n=2 hole states of Co-like xenon as a function of time.

An important question is raised by these calculations; namely, are the rates shown in Fig. 12 consistent with the enhanced bremsstrahlung emission rates calculated above? One indicator that they are is presented in Fig. 14. In this figure, a comparison is made between the power density, $P^{PI}$, absorbed in the calculation by the photoionizations that generate hole states to the bremsstrahlung power output density, $P^{Brems}$, that is calculated in the absence of an intense laser field, but that is enhanced by a factor of $4.5 \times 10^3$. This power output was calculated using the formula given in Eq. 23 of Ref.[12],

$$P^{Brems} \equiv n_i W(\nu) d\nu = \frac{128\pi^2}{3\sqrt{3}} n_i \alpha^3 Z^2 \left(n_e a_0^3\right) \left(\frac{E_0}{Ryd}\right)^{-1/2} d\nu g_{ff} Ryd, \tag{108}$$

where $\alpha \equiv e^2/(\hbar c)$, $a_0 = \hbar^2/(m_0 e^2)$, $Ryd \equiv e^2/(2a_0)$. The power output was calculated over a bandwidth, $d\nu$, of 6 keV from electrons whose energies were set at 40 keV, i.e., $P^{Brems}$ was approximated by setting $g_{ff} \cong 1$, $E_0 = 4 \times 10^4$ eV, and $\hbar d\nu = 6$ keV in this formula.

The calculated photoionization power input into the plasma is given by

$$P^{PI} = \sum_{\mu,\nu} n_\nu W^{PI}_{\mu \leftarrow \nu} \left(E_\mu - E_\nu\right), \tag{109}$$

where $E_\mu$ and $E_\nu$ are the energies of hole states and ground states respectively, $n_\nu$ are ground state population densities, and $W^{PI}_{\mu \leftarrow \nu}$ are the photoionization rates that connect them to the hole states. As expected from Fig. 11, the photoionization power input peaks slightly

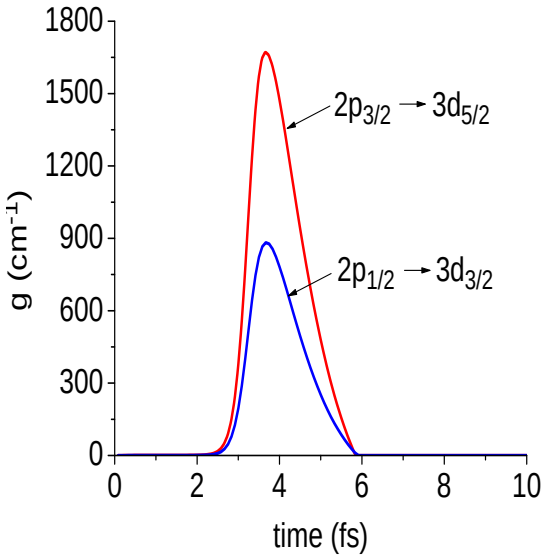


FIG. 13. The calculated gain coefficients as a function of time for the two hole-state radiative transitions shown.

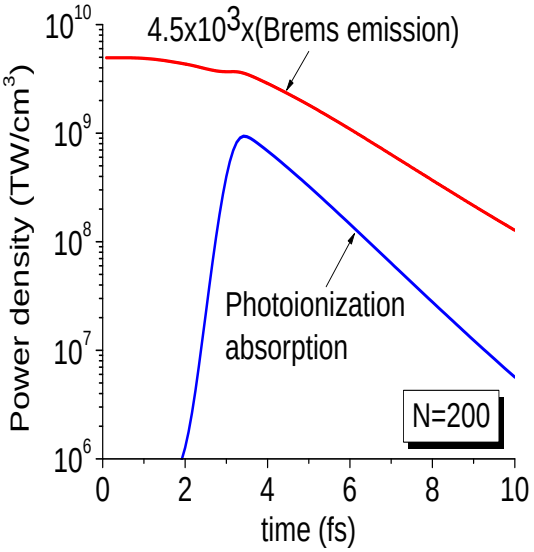


FIG. 14. The calculated power input, $P^{PI}$, to the cluster due to photoionization absorption as a function of time as compared to the bremsstrahlung power output, $P^{Brems}$, derived in the absence of a laser field, but enhanced by a factor of $4.5 \times 10^3$.

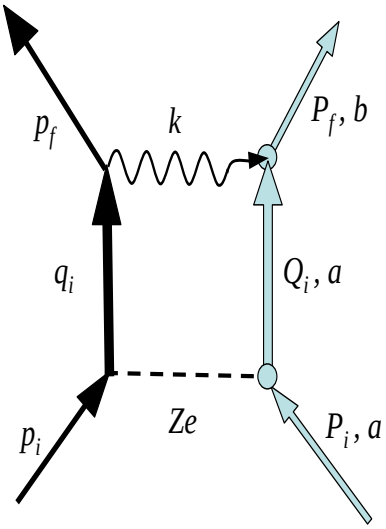


FIG. 15. A Feynman diagram, yet to be computed, of an electron scattering induced enhanced photoionization.

before the time of peak gain and at a time near when the peak value of the Ni-like ground state population is reached. Fig. 13 suggests that if an enhanced bremsstrahlung emission of the strength shown in Fig. 14 takes place, it can provide the needed photon flux to create the hole-state population inversions seen in the experiments.

## VI. SUMMARY AND CONCLUSIONS

In experiments in which KrF laser radiation was focused onto a cluster of xenon atoms at peak intensities $\gtrsim 10^{19}$ W/cm$^2$, hole states within the M-shell ionization stages of xenon were generated; i.e., emissions that result from the filling of these n=2 hole states were prominant in the recorded x-ray spectra between 2.5 and 3 $\mathring{A}$ as were amplified line emissions. A model, recently constructed to analyze the femtosecond cluster dynamics behind these amplifications[8, 9], assumed that the n=2 hole states were generated by photoionizations. It was found that large photon fluxes were needed in order to generate the gain coefficients that were measured in the experiments. More flux was needed, for example, than is produced by Bethe-Heitler bremsstrahlung, which is calculated in the absence of intense laser fields. Recent work[2], on the other hand, has predicted a four or more order of magnitude increase in bremsstrahlung emission rates when (1) it takes place in the presence of intense laser fields, (2) it is at the laser frequency, and (3) it has intensities that are $\lesssim 10^{17}$ W/cm$^2$. In this case, energy is predicted to be taken from the laser field and converted into enhanced bremsstrahlung emissions.

In this paper, the theory of Ref.[2] was first extended ($\eta_0 \sim 0.1$) and then extrapolated ($\eta_0 \to 1$) to higher laser harmonics of relevance to the calculation of the photoionization rates employed in Refs.[8–10]. By virtue of their dependence on Bessel functions, these high laser harmonic bremsstrahlung emissions were found to require laser intensities: $\gtrsim 10^{19}$ W/cm$^2$. Thus, this requirement on laser intensity plays an important role both (1) in rapidly stripping all N-shell electrons from a xenon atom in on the order of a femtosecond[8] and (2) in exceeding (by extrapolation) the intensity threshold that would be needed to reach a three to four order of magnitude enhancement of the bremsstrahlung emissions at energies above 5.6 keV. Moreover, it was then shown that a four order of magnitude increase in the power density output of Bethe-Heitler bremsstrahlung emission was consistent with (i.e., was much greater than) the photoionization power density inputs that were needed to produce the gains seen experimentally.

While this power input and output comparison is encouraging, it does not replace the need for a direct experimental verification of this speculated upon enhanced bremsstrahlung emission. However, experiments to confirm such enhancements must take into account the predicted reabsorption of these emissions through inner-shell photoionization processes,

especially if these processes occur by means of the process depicted by the Feynman diagram shown in Fig. 15. In this figure, state, a, represents the ground state of a xenon ion and state, b, represents a hole state. In this photoionization scattering process, both emission and absorption are virtual processes in the sense that no radiation transport per se takes place.

label command.

label command. the

**Appendix A: Matrix Element Evaluations**

Four traces defined by:

$$
\begin{aligned}
F_{r1} &= Tr\Big\{\tilde{\gamma}^{\mu}\Big((q_f\tilde{\gamma})+m_0\Big)\tilde{\gamma}^{0}\Big((p_i\tilde{\gamma})+m_0\Big)\tilde{\gamma}^{0}\Big((q_f\tilde{\gamma})+m_0\Big)\tilde{\gamma}_{\mu}\Big((p_f\tilde{\gamma})+m_0\Big)\Big\},\\
F_{r2} &= Tr\Big\{\tilde{\gamma}^{0}\Big((q_i\tilde{\gamma})+m_0\Big)\tilde{\gamma}^{\mu}\Big((p_i\tilde{\gamma})+m_0\Big)\tilde{\gamma}_{\mu}\Big((q_i\tilde{\gamma})+m_0\Big)\tilde{\gamma}^{0}\Big((p_f\tilde{\gamma})+m_0\Big)\Big\},\\
F_{r3} &= Tr\Big\{\tilde{\gamma}^{0}\Big((q_i\tilde{\gamma})+m_0\Big)\tilde{\gamma}^{\mu}\Big((p_i\tilde{\gamma})+m_0\Big)\tilde{\gamma}^{0}\Big((q_f\tilde{\gamma})+m_0\Big)\tilde{\gamma}_{\mu}\Big((p_f\tilde{\gamma})+m_0\Big)\Big\},\\
F_{r4} &= Tr\Big\{\tilde{\gamma}^{\mu}\Big((q_f\tilde{\gamma})+m_0\Big)\tilde{\gamma}^{0}\Big((p_i\tilde{\gamma})+m_0\Big)\tilde{\gamma}_{\mu}\Big((q_i\tilde{\gamma})+m_0\Big)\tilde{\gamma}^{0}\Big((p_f\tilde{\gamma})+m_0\Big)\Big\},
\end{aligned}
\tag{A1}
$$

enter into the approximate evaluation of $|S_{rs}^{fi}|^2$,where $q_i = p_i - k' + rk$ and $q_f = p_f + k' - rk$. These traces are computed in Ref. [1] for the case $r = s = 0$:

$$
\begin{aligned}
F_1 &\equiv 16\Big\{m_0^4 + \Big((p_i\tilde{p}_f)+(k'\tilde{p}_i)+(k'p_f)\Big)m_0^2 - (k'p_f)(k'\tilde{p}_i)\Big\},\\
F_2 &= 16\Big\{m_0^4 + \Big((p_i\tilde{p}_f)-(k'\tilde{p}_f)-(k'p_i)\Big)m_0^2 - (k'p_i)(k'\tilde{p}_f)\Big\},\\
F_3 &= -8\Big\{m_0^4 + 2\Big((p_i\tilde{p}_f)-(E_f+E_i)^2+\omega'^2\Big)m_0^2 + 2E_f^2(k'\tilde{p}_i)\\
&\qquad -2E_i^2(k'\tilde{p}_f) + (p_ip_f)^2 + (p_i\tilde{p}_f)^2 + (p_ip_f)(k'p_i) + (p_i\tilde{p}_f)(k'\tilde{p}_i)\\
&\qquad -(p_i\tilde{p}_i)(p_f\tilde{p}_f) - (p_ip_f)(k'p_f) - (p_i\tilde{p}_f)(p_i\tilde{p}_f)\Big\},\\
F_4 &= F_3,
\end{aligned}
\tag{A2}
$$

and, when $r \neq 0$, they are approximately given by

$$
\begin{aligned}
F_{r1} &= F_1 - 16(kp_f)(k\tilde{p}_i)r^2 - 16r\Big\{\Big((k\tilde{p}_i)+(kp_f)+2(k'k)\Big)m_0^2\\
&\qquad -(k'p_f)(k\tilde{p}_i) - (k'\tilde{p}_i)(kp_f) + (p_i\tilde{p}_f)(k'k)\Big\},\\
F_{r2} &= F_2 - 16(kp_i)(k\tilde{p}_f)r^2 + 16r\Big\{\Big((k\tilde{p}_f)+(kp_i)-2(k'k)\Big)m_0^2
\end{aligned}
$$

$$+(k'p_i)(k\tilde{p}_f)+(k'\tilde{p}_f)(kp_i)-(p_i\tilde{p}_f)(k'k)\Big\},$$

$$F_{r3}=F_3-8r\Big\{\Big(2\omega^2 r-4\omega'\omega+(k\tilde{p}_f)-(k\tilde{p}_i)\Big)m_0^2$$
$$+(p_i\tilde{p}_f)(k\tilde{p}_f)-(p_i\tilde{p}_f)(k\tilde{p}_i)+(p_i\tilde{p}_i)(k\tilde{p}_f)-(p_f\tilde{p}_f)(k\tilde{p}_i)$$
$$+(p_ip_f)(kp_f)-(p_ip_f)(kp_i)+2(p_ip_f)(k'k)\Big\},$$

$$F_{r4}=F_{r3}. \tag{A3}$$


## ACKNOWLEDGMENTS

Work supported by DOE/NNSA under contract DENA0000168, and by NRL under the 6.1 base program.


---


[1] W. Greiner and J. Reinhardt, *Quantum Electrodynamics* (Springer-Verlag, Berlin, 1992).

[2] A. A. Lebed and S. P. Roshchupkin, Phys. Rev. A **81**, 033413 (2010).

[3] S. P. Roshchupkin, Laser Physics **6**, 837 (1996).

[4] A. A. Lebed and S. P. Roshchupkin, Eur. Phys. J. D **53**, 113 (2009).

[5] A. Florescu and V. Florescu, Phys. Rev. A **61**, 033406 (2000).

[6] M. V. Fedorov, *Atomic and Free Electrons in a Strong Light Field*, (World Scientific Publishing Co., Singapore, 1997).

[7] A. B. Borisov, E. Racz, P. Zhang, J. C. McCorkindale, S. F. Khan, S. Poopalasingam, J. Zhao, and C. K. Rhodes, J. Phys. B: At. Mol. Opt. Phys. **41**, 105602, (2008) and references 1 through 7 cited therein.

[8] Tz. B. Petrova, K. G. Whitney, and J. Davis, J. Phys. B: At. Mol. Opt. Phys. **43**, 025601 (2010); **44**, 125601 (2011).

[9] J. Davis, K. G. Whitney, Tz. B. Petrova, and G. M. Petrov, High Energy Density Phys., 8, 238 (2012)].

[10] Tz. B. Petrova, J. Davis, K. G. Whitney, and G. M. Petrov, High Energy Density Phys., 8, 209 (2012)].

[11] M. A. Duguay and P. M. Rentzepis, Appl. Phys. Lett. **10**, 350 (1967).

[12] W. J. Karzas and R. Latter, The Astrophysical Journal, Supplement Series **55**, 167 (1961).

.